2-Step Phase Rotation Estimation for Low-PAPR Signal Transmission using Blind Selected Mapping

Amnart Boonkajay* and Fumiyuki Adachi†
Research Organization of Electrical Communication (ROEC), Tohoku University
2-1-1 Katahira, Aoba-ku, Sendai, Miyagi, 980-8577 Japan
E-mail: *amnart@riec.tohoku.ac.jp, †adachi@ecei.tohoku.ac.jp

***Abstract*—Blind selected mapping (blind SLM) can effectively reduce the peak-to-average power ratio (PAPR) of both orthogonal frequency division multiplexing (OFDM) and single-carrier (SC) signals without side-information transmission. In typical blind SLM, maximum likelihood (ML) estimation is applied to find the de-mapping phase rotation sequence which gives the lowest Euclidean distance among all possible sequences, resulting in very high computational complexity. In this paper, we introduce a novel low-complexity 2-step estimation suitable for blind SLM. In the first step, the phase rotation sequence achieving the lowest Euclidean distance is searched by using the Viterbi algorithm. In the second step, verification and correction are carried out to choose a phase rotation sequence stored in the codebook, which has the lowest Hamming distance from the estimated sequence in the first step. It is confirmed by computer simulation that our proposed 2-step estimation achieves similar BER performance to the transmission without SLM and the transmission with blind SLM with the conventional ML estimation, but the proposed estimation technique requires much less complexity.**

***Index Terms*—OFDM, DFT-precoded OFDM, PAPR**

I. Introduction

High peak-to-average power ratio (PAPR) signal causes a problem of low amplification efficiency in power amplifier (PA), especially when operating at high carrier frequency e.g. millimeter wave [1]. Orthogonal frequency division multiplexing (OFDM) waveform generally has higher PAPR than single-carrier (SC) waveform [2]. However, PAPR of SC waveform increases due to high-level data modulation and when the SC signal is generated by mean of discrete Fourier transform (DFT)-precoded OFDM [3]. Among various PAPR reduction techniques, selected mapping (SLM) [4] is well-known as a simple PAPR reduction method which requires lower computational complexity at the transmitter than partial transmit sequence (PTS) [5]. SLM selects the waveform with the lowest PAPR from multiple phase-rotated candidates. SLM for OFDM [4] and DFT-precoded OFDM [6] can reduce the PAPR effectively but requires side-information (e.g. selected phase sequence number) transmission.

SLM without side-information transmission (blind SLM) techniques based on a modification of phase rotations [7-8] are attractive since the average transmit power remains the same as that of original OFDM (or SC). However, [7] considers continuous set of phase rotations, which results in large number of candidates in phase rotation estimation at the receiver. The blind SLM in [8] introduces a discrete phase rotation set, but its transmission performance degrades when using high-level data modulation. Recently, we have shown in [9] that blind SLM using phase rotation sequences randomly generated from a discrete set $\{1, e^{i2\pi/3}, e^{i4\pi/3}\}$ achieves low PAPR similar to the conventional SLM [6] with no significant bit-error rate (BER) degradation even in high-level modulation. Although the SC signal transmission is considered in [9], it will be shown in this paper that the blind SLM in [9] can also be applied to OFDM signal.

Meanwhile, phase rotation sequence estimation at the receiver for blind SLM in [7-9] employs maximum likelihood (ML) estimation. ML estimation in [9] searches the mapping sequence used at the transmitter by computing the Euclidean distance between the de-mapped signal and original data-modulated signal constellation (before mapping at the transmitter) among all possible phase sequences. The de-mapping sequence which gives the lowest Euclidean distance is chosen for succeeding data demodulation. Since the ML is based on exhaustive search, it has high computational complexity and is impractical when the number of sequences is large.

In this paper, we introduce a novel 2-step phase rotation sequence estimation for blind SLM in order to realize low-PAPR waveform and low-complexity receiver. Both OFDM and DFT-precoded OFDM are considered (hereinafter we denote DFT-precoded OFDM as SC for simplicity). The proposed estimation technique can be briefly described as follows. In the first step, the phase rotation sequence giving the lowest Euclidean distance is searched by using Viterbi algorithm [10]. In the second step, verification and correction are carried out to choose a phase rotation sequence which is stored in the codebook and has the lowest Hamming distance

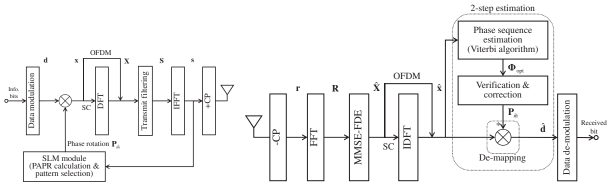

(a) Transmitter (b) Receiver

Fig. 1. Transceiver model.

from the estimated sequence obtained from the first step. Simulation results are provided to show that the proposed 2-step estimation achieves similar BER compared to the ML estimation but with much less complexity.

II. Principle of blind SLM

The transmitter equipped with blind SLM is shown in Fig. 1(a). For simplicity, single-input single-output (SISO) point-to-point block transmission is assumed. N_c subcarriers are available to contain data. The transmit signals and processing techniques are represented by row vectors and matrices, respectively. Let $\mathbf{d} = [d(0), d(1), \ldots, d(N_c-1)]^T$ denote N_c-length data-modulated transmit vector. The transmit block is then phase rotated by the selected phase rotation matrix $\mathbf{P}_{\hat{m}} = diag[P_{\hat{m}}(0), P_{\hat{m}}(1), \ldots, P_{\hat{m}}(N_c-1)]$, yielding the phase-rotated time-domain signal $\mathbf{x} = \mathbf{P}_{\hat{m}}\mathbf{d}$. The phase rotation sequence $\mathbf{P}_{\hat{m}}$ is an $N_c \times N_c$ diagonal matrix which is selected to minimize the PAPR of transmit waveform, where the selection criterion can be expressed as [6,9]

$$\mathbf{P}_{\hat{m}_j} = \begin{cases} \arg \min\limits_{m=0\sim M-1} \text{PAPR}(\mathbf{F}_{N_c}^H \mathbf{H}_T \mathbf{P}_m \mathbf{d}) \text{ for OFDM}, \\ \arg \min\limits_{m=0\sim M-1} \text{PAPR}(\mathbf{F}_{N_c}^H \mathbf{H}_T \mathbf{F}_{N_c} \mathbf{P}_m \mathbf{d}) \\ \qquad\qquad\qquad \text{for SC}, \end{cases} \tag{1}$$

where $\mathbf{F}_{N_c}$ and $\mathbf{F}_{N_c}^H$ represent the DFT and inverse DFT (IDFT), respectively. A codebook consisting of M different phase rotation sequences $\mathbf{P}_m = diag[P_m(0), \ldots, P_m(N_c-1)]$, $m = 0 \sim M-1$ is defined, where the phase rotation sequences are randomly generated as $P_m(n) \in \{1, e^{i2\pi/3}, e^{i4\pi/3}\}$, $n = 0 \sim N_c-1$, $m = 1 \sim M-1$ except the first sequence as $P_0(n) = 1$, $n = 0 \sim N_c-1$. Note that the above polyphase rotation patterns are not optimal but sufficient for realizing the blind phase rotation sequence estimation. PAPR of a particular N_c-length time-domain transmit block $\mathbf{s} = [s(0), s(1), \ldots, s(N_c-1)]^T$ is

$$\text{PAPR}(\mathbf{s}) = \frac{\max\{|s(n)|^2, n = 0, \frac{1}{V}, \frac{2}{V}, \ldots, N_c-1\}}{\frac{1}{N_c}\sum_{n=0}^{N_c-1}|s(n)|^2}, \tag{2}$$

where V is oversampling factor. Transmit filtering matrix $\mathbf{H}_T = diag[H_T(0), \ldots, H_T(N_c-1)]$ is assumed to be an ideal rectangular filter, i.e. $H_T(k)$=1 if $k < N_c$ and $H_T(k)$=0 elsewhere.

In the case of SC transmission, the phase rotated transmit block $\mathbf{x}$ is transformed into frequency domain by N_c-point DFT, yielding the frequency components $\mathbf{X} = [X(0), X(1), \ldots, X(N_c-1)]^T$ as $\mathbf{X} = \mathbf{F}_{N_c}\mathbf{x}$ for SC transmission and $\mathbf{X} = \mathbf{x}$ for OFDM transmission, respectively. $\mathbf{F}_{N_c}$ is shown by defining $i = \sqrt{-1}$ as

$$\mathbf{F}_{N_c} = \frac{1}{\sqrt{N_c}} \begin{bmatrix} 1 & 1 & \cdots & 1 \\ \vdots & \vdots & \ddots & \vdots \\ 1 & e^{\frac{-i2\pi(N_c-1)(1)}{N_c}} & \cdots & e^{\frac{-i2\pi(N_c-1)(N_c-1)}{N_c}} \end{bmatrix}. \tag{3}$$

The frequency-domain signal $\mathbf{X}$ is then multiplied by the transmit filtering and subcarrier mapping matrix, yielding the frequency-domain filtered signal $\mathbf{S} = \mathbf{H}_T\mathbf{X}$ where $\mathbf{S} = [S(0), S(1), \ldots, S(N_c-1)]^T$. After that, $\mathbf{S}$ is transformed back into time domain by N_c-point IDFT matrix $\mathbf{F}_{N_c}^H$. The selected transmit signal based on SLM can be summarized as

$$\mathbf{s} = \begin{cases} \mathbf{F}_{N_c}^H \mathbf{H}_T \mathbf{P}_{\hat{m}} \mathbf{d} & \text{for OFDM}, \\ \mathbf{F}_{N_c}^H \mathbf{H}_T \mathbf{F}_{N_c} \mathbf{P}_{\hat{m}} \mathbf{d} & \text{for SC}. \end{cases} \tag{4}$$

IDFT can be changed to inverse fast Fourier transform (IFFT) if N_c is a power of 2. Finally, the last N_g samples of transmit block are copied as a cyclic prefix (CP) and inserted into the guard interval (GI), then a CP-inserted signal block of $N_g + N_c$ samples is transmitted.

The receiver with phase rotation sequence estimation is illustrated by Fig. 1(b). The wireless channel is assumed to be a symbol-spaced L-path frequency-selective block fading channel, where its impulse response is

$$h(\tau) = \sum_{l=0}^{L-1} h_l \delta(\tau - \tau_l), \tag{5}$$

where h_l and τ_l are complex-valued path gain and time delay of the l-th path, respectively. Time-domain received signal vector $\mathbf{r} = [r(0), r(1), \ldots, r(N_c-1)]^T$ can be expressed by

$$\mathbf{r} = \sqrt{2E_s/T_s}\mathbf{h}\mathbf{s} + \mathbf{n}, \tag{6}$$

where E_s is symbol energy, and $\mathbf{n}$ is noise vector whose each element is zero-mean additive white Gaussian noise (AWGN) having the variance $2N_0/T_s$. T_s is symbol duration and N_0 is the one-sided noise power spectrum density. Channel response matrix $\mathbf{h}$ is a circulant matrix [6]. The received signal vector $\mathbf{r}$ is then transformed into frequency domain by N_c-point DFT (or FFT), obtaining the frequency-domain signal $\mathbf{R} = [R(0), \ldots, R(N_c-1)]^T$ as

$$\begin{aligned} \mathbf{R} &= \sqrt{2E_s/T_s}\mathbf{F}_{N_c}\mathbf{h}\mathbf{F}_{N_c}^H\mathbf{H}_T\mathbf{X} + \mathbf{F}_{N_c}\mathbf{n} \\ &= \sqrt{2E_s/T_s}\mathbf{H}\mathbf{H}_T\mathbf{X} + \mathbf{N} \end{aligned}, \tag{7}$$

where the frequency-domain channel response $\mathbf{H}$ is defined by $\mathbf{H} \equiv diag[H(0), \ldots, H(N_c-1)] = \mathbf{F}_{N_c}\mathbf{h}\mathbf{F}_{N_c}^H$.

FDE based on minimum mean-square error criterion (MMSE-FDE) is employed by multiplying the FDE matrix $\mathbf{W}_r = diag[W_r(0), \ldots, W_r(N_c-1)]$ to $\mathbf{R}$, yielding

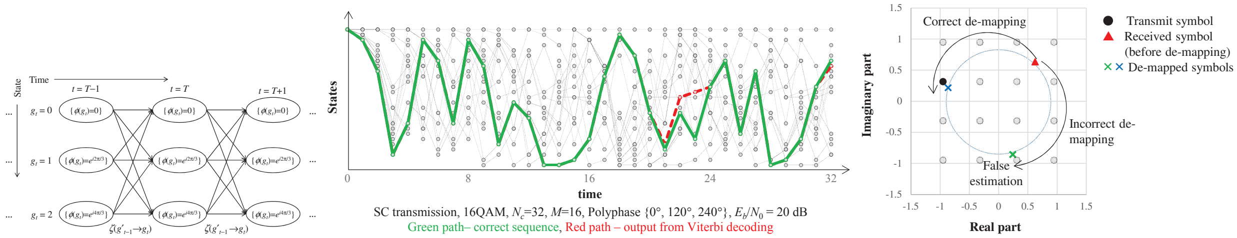

(a) Illustration of 3-state trellis (b) An example of trellis diagram with reduced branches (c) Estimation error in Viterbi algorithm

Fig. 2. Phase rotation sequence estimation using Viterbi algorithm.

the equalized signal $\hat{\mathbf{X}} = \mathbf{W}_r\mathbf{R}$. The FDE weight at the k-th frequency index is expressed by

$$W_r(k)=\frac{H^*(k)H_T(k)}{|H^*(k)H_T(k)|^2+(E_s/N_0)^{-1}}, \tag{8}$$

where $H(k)$ is the k-th element in the diagonal of $\mathbf{H}$, which corresponds to the frequency-domain channel gain at the k-th subcarrier.

After that, the received signal before de-mapping $\hat{\mathbf{x}} = [\hat{x}(0),\ldots,\hat{x}(N_c-1)]^T$ is obtained based on different transmission techniques. In SC transmission, $\hat{\mathbf{x}}$ is obtained by applying N_c-point IDFT to $\hat{\mathbf{X}}$, that is $\hat{\mathbf{x}} = \hat{\mathbf{X}}$ for OFDM and $\hat{\mathbf{x}} = \mathbf{F}^H_{N_c}\hat{\mathbf{X}}$ for SC. Note that the phase rotation due to SLM still remains in $\hat{\mathbf{x}}$. In general, the received symbol vector $\hat{\mathbf{d}} = [\hat{d}(0),\hat{d}(1),\ldots,\hat{d}(N_c-1)]^T$ is obtained by employing de-mapping, i.e. multiplying $\hat{\mathbf{x}}$ by $\mathbf{P}^H_{\hat{m}}$, but it requires side-information transmission. We have introduced an ML estimation for estimating the selected phase rotation sequence $\mathbf{P}_{\tilde{m}}$ [9], which its index $\tilde{m}$ can be expressed by

$$\tilde{m} = \arg\min_{\substack{m=0\sim M-1,\\ \mathbf{d}\in\Psi_{\text{mod}}}} \left(\epsilon = \left\|\mathbf{P}^H_m\hat{\mathbf{x}}-\mathbf{d}\right\|\right), \tag{9}$$

where $\|\cdot\|$ represents the Euclidean norm and Ψ_{mod} is the original data-modulated constellation. Note that $\mathbf{d}$ is not considered as an output in this paper. Eq. (9) needs to compute the Euclidean norm for all possible de-mapping sequences and all possible data-modulated symbols, resulting in high complexity when M is large.

III. 2-STEP PHASE ROTATION SEQUENCE ESTIMATION

A. Viterbi algorithm

The objective function ϵ in (9) can be rewritten by ignoring the codebook and assuming that Φ_{SLM} is a set of possible rotation patterns $\{1, e^{i2\pi/3}, e^{i4\pi/3}\}$ as

$$\arg\min_{\substack{\phi(t)\in\Phi_{\text{SLM}},\\ d\in\Psi_{\text{mod}}}} \left(\epsilon = \sum_{t=0}^{N_c-1}\frac{1}{N_c}\left|\phi^*(t)\hat{x}(t)-d\right|^2\right). \tag{10}$$

Then, ϵ at time index $t=T, 0\le T\le N_c-1$ is expressed by

$$\begin{aligned}\epsilon(T) &= \sum_{t=0}^{T}\frac{1}{N_c}\min_{\substack{\phi(t)\in\Phi_{\text{SLM}},\\ d\in\Psi_{\text{mod}}}}\left|\phi^*(t)\hat{x}(t)-d\right|^2 \\ &= \epsilon(T-1)+\frac{1}{N_c}\min_{\substack{\phi(T)\in\Phi_{\text{SLM}},\\ d\in\Psi_{\text{mod}}}}\left|\phi^*(T)\hat{x}(T)-d\right|^2\end{aligned} \tag{11}$$

We can search an optimal phase rotation sequence $\phi_{\text{opt}}(t), t=0\sim N_c-1$ by using Viterbi algorithm [10]. The first term and second term in (11) are considered as path metric at time t and state g, $\epsilon(g_t)$, and branch metric from state g' at time t to state g at time $t+1$, $\zeta(g'_t\to g_{t+1})$, respectively, in the Viterbi algorithm. An example of trellis diagram assuming $G_{\max}$=3 states, i.e. $g_t = 0\sim 2$, is shown by Fig. 2(a).

The initial path metric for each state at time $t=-1$ is set as $\epsilon(g_{-1}) = 0$ for all $g = 0 \sim G_{\max}-1$. At a particular time index t where $0\le t\le N_c-1$, the branch metric from state g' at time t to state g at time $t+1$ is expressed by

$$\zeta(g'_t\to g_{t+1})=\frac{1}{N_c}\min_{d\in\Psi_{\text{mod}}}\left|\phi^*(g_{t+1})\hat{x}(t+1)-d\right|^2, \tag{12}$$

where $\phi(g_{t+1})$ is the phase rotation at state g and time $t+1$. Then the path metric entering state g_{t+1} is selected by the following criterion.

$$\epsilon(g_{t+1}) = \min_{g'_t=0\sim G_{\max}}\left(\epsilon(g'_t)+\zeta(g'_t\to g_{t+1})\right). \tag{13}$$

Note that (12)-(13) are repeated until $t=N_c-1$. Once the path metric calculation is done until $t=N_c-1$, the surviving path metric which provides an optimal state number $g_{t,\text{opt}}$ and the optimal sequence $\phi_{\text{opt}}(t) = \phi(g_{t,\text{opt}}), t=0\sim N_c-1$ can be determined by backward computation as follows.

$$g_{N_c-1,\text{opt}} = \arg\min_{g_{N_c-1}=0\sim G_{\max}-1}\epsilon(g_{N_c-1}), \tag{14}$$

$$g_{t',\text{opt}} = \arg\min_{g_{t'}=0\sim G_{\max}-1}\left(\epsilon(g_{t'})+\zeta(g_{t'}\to g_{t'+1,\text{opt}})\right), \tag{15}$$

where $t' = N_c-2, N_c-3,\ldots,0$. We set $G_{\max}$=3^3=27 in this paper, meaning that the phase rotation patterns in a particular state g_t is determined as a set of phase patterns at $t-2$, $t-1$ and t. The above algorithms can be used without modifications except the initialization should be done at t=2. An increasing of $G_{\max}$ leads to an increasing of branches, where the redundant branches and states (i.e. the branches and states which do not exist in the codebook) can be removed prior to estimation. This can improve the accuracy of estimation but increases the complexity due to many surviving branches and states. A study about setting the value of $G_{\max}$ is left as our future works. Fig. 2(b) shows an example of 27-state

TABLE I
SIMULATION PARAMETERS.

Transmitter	Modulation	16QAM, 64QAM
	FFT/IFFT block size	N_c = 256
	Cyclic prefix length	N_g = 16
	Phase sequence type	Random polyphase
Channel	Fading type	Frequency-selective 16-path block Rayleigh
Receiver	Channel estimation	Ideal
	FDE	MMSE-FDE

trellis with N_c=32 and M=16, where the branches and states are partially removed.

However, the estimated $\phi_{\text{opt}}(t), t = 0 \sim N_c - 1$ still contains error due to frequency-selective fading and noise. This is also shown in Fig. 2(b) and assuming the average received bit energy-per-noise power spectrum density (E_b/N_0) equals 20 dB that the surviving path (red dash line) is different from the actual phase rotation sequence used at the transmitter (green solid line). The cause of error can be described by referring Fig. 2(c), which shows the received signal and the de-mapped signals at t=22. It is seen that the received symbol with incorrect de-mapping gives lower Euclidean distance from original 16QAM constellations than that of correct de-mapping. The Viterbi algorithm is aiming at selecting the path with the lowest mean-square error (MSE), hence the incorrect sequence is selected as a surviving path instead. We introduce verification and correction as the second step for reducing the above error occurred in Viterbi decoding.

B. Verification & correction

Fig. 3(b) also shows that the estimated phase sequence obtained from Viterbi decoding contains errors on few samples only when the received E_b/N_0 is sufficiently high. These errors can be corrected by checking the similarity of output from Viterbi decoding and the available sequences in the codebook. Here, Hamming distance is used as an indicator for checking the similarity since the difference in rotation angle does not affect the data detection error.

Let $\mathbf{\Phi}_{\text{opt}} = diag[\phi_{\text{opt}}(0), \phi_{\text{opt}}(1), \ldots, \phi_{\text{opt}}(N_c - 1)]$ denote the phase rotation sequence matrix obtained from the Viterbi decoding. The estimated phase rotation sequence for de-mapping $\mathbf{P}_{\tilde{m}} = diag[P_{\tilde{m}}(0), P_{\tilde{m}}(1), \ldots, P_{\tilde{m}}(N_c - 1)]$ with the corresponding sequence index $\tilde{m}$ can be determined by

$$\tilde{m} = \arg \min_{m=0\sim M-1} d\left(\mathbf{\Phi}_{\text{opt}}, \mathbf{P}_m\right), \tag{16}$$

where $\mathbf{P}_m = diag[P_m(0), \ldots, P_m(N_c - 1)]$ is the m-th phase rotation sequence in the codebook and $d(\mathbf{A}, \mathbf{B})$ represents the Hamming distance between matrices $\mathbf{A}$ and $\mathbf{B}$. Finally, the de-mapped symbols vector is obtained by $\hat{\mathbf{d}} = \mathbf{P}_{\tilde{m}}^H \hat{\mathbf{x}}$.

IV. PERFORMANCE EVALUATION

Numerical and simulation parameters are summarized in Table I. Channel coding is not considered. The performance of blind SLM with ML estimation [9] is also done as a conventional scheme for comparison.

A. PAPR vs Computational Complexity

Computational complexity is defined by counting the number of real-valued multiplication and real-valued addition operations. Table II shows the computational complexity of ML estimation and 2-step estimation with N_{mod} representing modulation level (4 for 16QAM and 6 for 64QAM). It is seen that the complexity of ML estimation is a function of M. On the other hand, computational complexity of 2-step estimation is almost independent from M and is an order of N_{trellis}, where $N_{\text{trellis}} \leq (81 \times (N_c - 2)) + 27$ if G_{max}=27. In addition, since we are considering only the complexity of phase rotation sequence estimation which is the major part of the blind SLM receiver, the computational complexity shown in Table II is identical for both OFDM and SC transmissions.

Fig. 3(a) shows the $\text{PAPR}_{0.1\%}$ versus total computational complexity of OFDM and SC, respectively. $\text{PAPR}_{0.1\%}$ is defined as the PAPR value at the complementary cumulative distribution function (CCDF) equals 10^{-3}, while the $\text{PAPR}_{0.1\%}$ of conventional SC(OFDM) are 8.8(11.3) dB for 16QAM and 9.1(11.3) dB for 64QAM, respectively (note that the PAPR of OFDM is irrespective of the modulation level [3,6]). Total computational complexity is defined by estimating that the complexity of a real-valued multiplication operation is 3 times of real-valued addition, then counting the total number of real-valued additions [11]. Transmission scheme with the performance trade-off mark in the bottom-left of Fig. 4(a) means the transmission scheme which achieves low PAPR with low-complexity phase rotation sequence estimation.

PAPR can be reduced when M increases, but the computational complexity also increases. The complexity of ML estimation drastically increases when M increases. On the other hand, the complexity of 2-step estimation is much lower than that of the ML when $M \leq 256$. For example, when M=2048 and assuming 16QAM modulation, SC using blind SLM and 2-step detection achieves the PAPR of 5.5 dB (i.e., 3.3 dB reduction), OFDM using blind SLM and 2-step detection achieves the PAPR of 6.8 dB (i.e., 4.5 dB reduction), while the complexity of phase rotation estimation is only 5% of the ML estimation. Therefore, the use of blind SLM and 2-step estimation can achieve very low-PAPR signal by

TABLE II
COMPUTATIONAL COMPLEXITY

	No. of real-valued multiplications	No. of real-valued additions
ML estimation	$M \times \left(N_c \times (4+2(2^{N_{\text{mod}}}))+1\right)$	$M \times N_c \times \left(3+3(2^{N_{\text{mod}}})\right)$
2-step estimation	$N_{\text{trellis}} \times \left(6+2(2^{N_{\text{mod}}})\right)$	$\left(N_{\text{trellis}} \times \left(3+3(2^{N_{\text{mod}}})\right)\right) + (M \times N_c)$

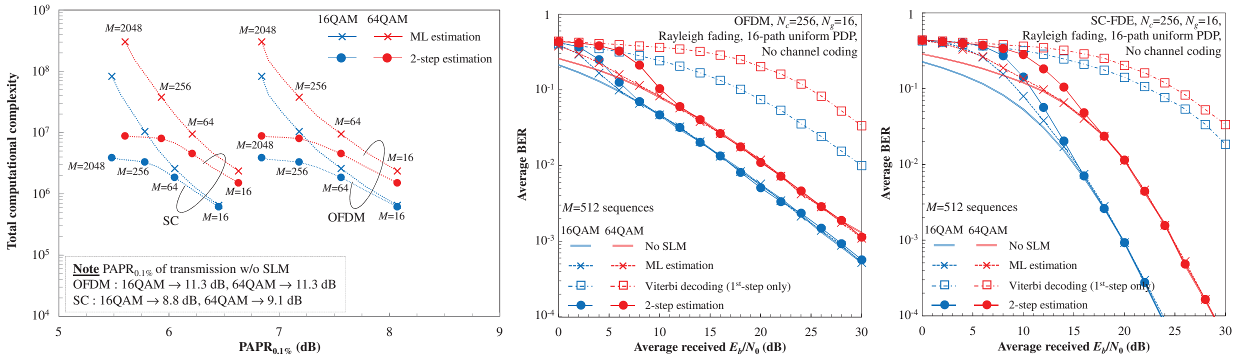

(a) PAPR versus computational complexity trade-off (b) BER (OFDM transmission) (c) BER (SC transmission)

Fig. 3. Simulation results.

using large M without causing high-complexity problem at the receiver.

B. BER Performance

Figs. 3(b) and 3(c) show the BER of OFDM and SC using blind SLM, respectively, as a function of average received E_b/N_0 where $E_b/N_0{=}(1/N_{\rm mod})(E_s/N_0)(1+N_g/N_c)$. BER of conventional SC and OFDM and those of blind SLM using ML estimation are available for comparison. The number of phase rotation sequences is M=512.

Firstly, it is seen in both 16QAM and 64QAM transmissions that the BER of phase rotation sequence estimation using only Viterbi decoding is the worst due to an estimation error described in Sect. III-B. However, both ML and 2-step estimations achieve similar BER performance compared to those of conventional SC and OFDM. This is because the use of FDE can effectively mitigate the spectrum distortion occurred in the received signal and accordingly improving the accuracy of phase rotation sequence estimation. More importantly, the second step (verification and correction) can effectively mitigate the estimation error occurred when using only Viterbi decoding. The 2-step estimation achieves slightly worse BER than ML estimation when E_b/N_0 is low. This is because the noise makes the estimation error in Viterbi algorithm become more severe, and consequently verification and correction cannot find the correct phase rotation sequence from the codebook. Meanwhile, although 2-step estimation is employed, there is no significant BER degradation compared to no SLM case when E_b/N_0 is sufficiently high. This concludes that the 2-step estimation can be used for blind SLM, while its complexity is much lower than ML estimation.

V. Conclusion

A 2-step phase rotation sequence estimation scheme for blind SLM was proposed. The proposed 2-step estimation employs Viterbi algorithm and then, carries out verification and correction for improving estimation accuracy. Computer simulation results confirmed that the 2-step estimation achieves similar BER performance compared to the conventional ML estimation with much lower computational complexity at the receiver. As a consequence, we can increase the number of phase rotation sequences for further lowering the PAPR.

Acknowledgment

This paper includes a part of results of “The research and development project for realization of the fifth-generation mobile communications system,” commissioned to Tohoku University by The Ministry of Internal Affairs and Communications (MIC), Japan.

References

[1] W. L. Chan and J. R. Long, “A 58-65 GHz Neutralized CMOS Power Amplifier with PAE above 10% at 1-V Supply,” *IEEE Journal of Solid-State Circuits*, Vol. 45, No. 3, pp. 554-564, Mar. 2010.

[2] H. G. Myung et al., “Single Carrier FDMA for Uplink Wireless Transmission,” *IEEE Veh. Technol. Mag.*, Vol. 1, No. 3, pp. 30-38, Sept. 2006.

[3] H. Ochiai, “On Instantaneous Power Distributions of Single-Carrier FDMA Signals,” *IEEE Wireless Commun. Lett.*, Vol. 1, No. 2, pp. 73-76, Jan. 2012.

[4] R. W. Bauml et al., “Reducing the Peak-to-Average Power Ratio of Multicarrier Modulation by Selected Mapping,” *IEEE Electron. Lett.*, Vol. 32, No. 22, pp. 2056-2057, Oct. 1996.

[5] R. J. Baxley and G. T. Zhou, “Comparison of Selected Mapping and Partial Transmit Sequence for Crest Factor Reduction in OFDM,” *Proc. IEEE Military Commun. Conference (MILCOM 2006)*, Washington D.C., USA, Oct. 2006.

[6] A. Boonkajay and F. Adachi, “Selected Mapping Technique for Reducing PAPR of Single-Carrier Signals,” *Wireless Commun. and Mobile Computing*, Vol. 16, No. 16, pp. 2509-2522, Nov. 2016.

[7] A. D. S. Jayalath and C. Tellambura, “SLM and PTS Peak-Power Reduction of OFDM Signals without Side Information,” *IEEE Trans. Wireless Commun.*, Vol. 4, No. 5, pp. 2006-2013, Sept. 2005.

[8] C. Siegl and R. F. H. Fischer, “Selected Mapping with Implicit Transmission of Side Information using Discrete Phase Rotations,” *Proc. Int. ITG Conference on Source and Channel Coding (SCC 2010)*, Siegen, Germany, Jan. 2010.

[9] A. Boonkajay and F. Adachi, “A Blind Polyphase Time-Domain Selected Mapping for Filtered Single-Carrier Signal Transmission,” *Proc. IEEE Veh. Technol. Conference (VTC 2016-Fall)*, Montreal, Canada, Sept. 2016.

[10] A. Viterbi, “Error Bound for Convolutional Codes and an Asymptotically Optimum Decoding Algorithm,” *IEEE Trans. Inform. Theory*, Vol. 13, No. 2, pp. 260-269, Apr. 1967.

[11] S. Arora and B. Barak,” *Computational Complexity: A Modern Approach*, Cambridge, 2009.